

ChemComm

Accepted Manuscript



This is an *Accepted Manuscript*, which has been through the Royal Society of Chemistry peer review process and has been accepted for publication.

Accepted Manuscripts are published online shortly after acceptance, before technical editing, formatting and proof reading. Using this free service, authors can make their results available to the community, in citable form, before we publish the edited article. We will replace this *Accepted Manuscript* with the edited and formatted *Advance Article* as soon as it is available.

You can find more information about *Accepted Manuscripts* in the [Information for Authors](#).

Please note that technical editing may introduce minor changes to the text and/or graphics, which may alter content. The journal's standard [Terms & Conditions](#) and the [Ethical guidelines](#) still apply. In no event shall the Royal Society of Chemistry be held responsible for any errors or omissions in this *Accepted Manuscript* or any consequences arising from the use of any information it contains.



Photoinduced electron transfer in porous organic salt crystals impregnated with fullerenes[†]

Received 00th January 20xx,
Accepted 00th January 20xx

Tetsuya Hasegawa,^a Kei Ohkubo,^{bc} Ichiro Hisaki,^a Mikiji Miyata,^a Norimitsu Tohnai^{*a} and Shunichi Fukuzumi^{*cd}

DOI: 10.1039/x0xx00000x

www.rsc.org/

Porous organic salt (POS) crystals composed of 9-(4-sulfophenyl)anthracene (SPA) and triphenylmethylamine (TPMA) were impregnated with fullerenes (C₆₀ and C₇₀), which were arranged in one dimensional close contact. POS crystals of SPA and TPMA without fullerenes exhibit blue fluorescence due to SPA, whereas the fluorescence was quenched in POS with fullerenes due to electron transfer from the singlet excited state of SPA to fullerenes.

Metal–organic frameworks (MOFs) have merited increasing attention as an interesting platform to design and develop artificial photosynthetic systems, because MOFs can contain light-harvesting and charge-separation units as well as catalytic units in a single crystal, providing the structural organization to integrate these units of artificial photosynthesis into a single crystal.¹ There are many examples of MOFs in which energy and electron transfer have been investigated by fixing the distance and orientation between chromophores, which were precisely determined by single crystal X-ray crystallography.^{2–10}

As compared with MOFs, porous organic salts (POSs) have advantage in terms of synthetic versatility, easier processing, more flexibility and better workability.^{11–15} In particular, POSs composed of ammonium cations and sulfonate anions have enabled various systematic design of resultant porous structures by changing the combination of ionic components using strong intermolecular interactions such as hydrogen bonds and electrostatic interactions.^{16,17} However, there has been no report on photoinduced

electron transfer in POS crystals.

We report herein the first example of efficient photoinduced electron transfer in POS crystals composed of 9-(4-sulfophenyl)anthracene (SPA) and triphenylmethylamine (TPMA) impregnated with fullerenes (C₆₀ and C₇₀) as revealed by femtosecond laser flash photolysis and electronic paramagnetic resonance (EPR) measurements. Fullerenes were chosen as electron acceptors, because they are known to undergo efficient electron-transfer reduction with small reorganization energies.¹⁸ The combination of SPA and TPMA was chosen in order to make enough space for accommodation of fullerenes in the porous structure.

SPA was synthesized according to the literature (see Electronic Supplementary Information (ESI[†])).¹⁹ The organic salt composed of SPA and TPMA yielded pale yellow needle crystal of SPA/TPMA suitable for X-ray crystallographic analysis from an *o*-dichlorobenzene solution. The X-ray crystal structure of SPA/TPMA in Fig. 1a revealed that the crystal had a porous structure, which was hierarchically constructed (Fig. S1 in ESI[†]). Four SPA molecules and four TPMA molecules assembled into tetrahedral supramolecular cluster via cubic-like charge-assisted hydrogen bond.²⁰ Anthracene moieties of SPA were jutting out in the tetrahedral direction and located around core structure. The tetrahedral clusters accumulated along *c*-axis by CH- π interaction between anthracene moieties and trityl group to form linear column structure differently from previous diamondoid structures.²¹ The

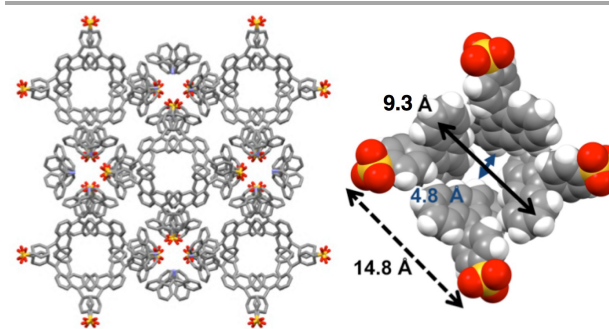


Fig. 1 Crystal structure of SPA/TPMA (left panel). The void space in SPA/TPMA (right panel).

^a Department of Material and Life Science, Graduate School of Engineering, Osaka University, Suita, Osaka 565-0871, Japan. E-mail: tohnai@mls.eng.osaka-u.ac.jp

^b Department of Applied Chemistry, Graduate School of Engineering, Osaka University, Suita, Osaka 565-0871, Japan.

^c Department of Chemistry and Nano Science, Ewha Womans University, Seoul 120-750, Korea. E-mail: fukuzumi@chem.eng.osaka-u.ac.jp

^d Faculty of Science and Technology, Meijo University, ALCA and SENTAN, Japan Science and Technology Agency (JST), Nagoya, Aichi 468-8502, Japan

[†] Electronic Supplementary Information (ESI) available: Experimental and spectral data. See DOI:

column structures were bundled by CH- π interactions between anthracene moieties to give a bowl-like void space among the columns. The void spaces were connected to lead to channel type porous structure having bottle-neck (Fig. S2 in ESI†). Recrystallization solvents were incorporated there but disordered.

The void space of SPA/TPMA from *o*-dichlorobenzene with the diameter of 9.3 Å (Fig. 1b) is capable to accommodate fullerenes. Recrystallizations of SPA/TPMA with C₆₀ and C₇₀ gave purple-red and red-brown needle crystals, respectively. X-ray studies revealed that the porous organic salts composed of SPA and TPMA were impregnated with fullerenes as shown in Fig. 2. The crystallographic parameters of SPA/TPMA, SPA/TPMA/C₆₀ and SPA/TPMA/C₇₀ are shown in Table S1 (ESI†). The void space is enlarged by impregnation of fullerenes to be 10.8 Å and 11.1 Å in SPA/TPMA/C₆₀ and SPA/TPMA/C₇₀, respectively (Fig. S3 in ESI†), because of comparatively weak interaction among the columns. This indicates the flexibility of the POS crystals. Moreover, the bottleneck in SPA/TPMA/C₆₀ and SPA/TPMA/C₇₀ is also expanded to be 6.6 Å and 7.2 Å, respectively. Consequently, the distance between fullerenes is getting closer in the porous structures.

The SPA/TPMA crystal exhibits fluorescence due to the SPA moiety under photoirradiation (Fig. 3).²² In contrast, the SPA/TPMA/C₆₀ and SPA/TPMA/C₇₀ exhibited no fluorescence probably because of electron transfer from the singlet excited state of SPA to the fullerene. The occurrence of the photoinduced electron transfer in SPA/TPMA/C₆₀ crystals was confirmed by femtosecond laser flash photolysis measurements. The observed transient absorption spectra are shown in Fig. 4, where the transient absorption band at 580 nm of SPA (¹SPA*) was observed upon femtosecond laser excitation and the decay is accompanied by increase in the new absorption band at 700 nm due to the radical cation of SPA (SPA⁺).²³ The concomitant formation of C₆₀⁻ was also observed at 1030 nm.¹⁸ Thus, photoinduced electron transfer

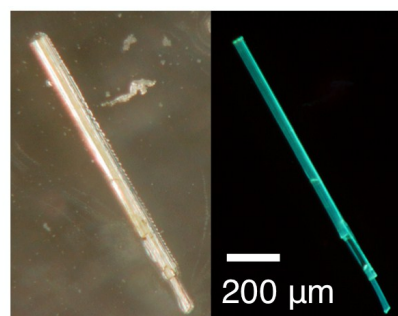


Fig. 3 Colour change of a SPA/TPMA crystal from *o*-dichlorobenzene under photoirradiation.

from ¹SPA* to C₆₀ occurred in SPA/TPMA/C₆₀ to produce the charge-separated (CS) state (SPA⁺/TPMA/C₆₀⁻).

The rate constant of photoinduced electron transfer from ¹SPA* to C₆₀ was determined from the fast decay of absorbance at 600 nm due to ¹SPA* to be $7.3 \times 10^{11} \text{ s}^{-1}$ (Fig. 5a). The decay time profile of absorbance at 700 nm due to SPA⁺ exhibited two components as shown in Fig. 5b, where the fast component afforded the rate constant of $7.3 \times 10^{11} \text{ s}^{-1}$, which agrees with the rate constant of electron transfer from ¹SPA* to C₆₀, and the slower component afforded the rate constant of $1.9 \times 10^{10} \text{ s}^{-1}$. This value is larger than the decay rate constant of C₆₀⁻ ($5.7 \times 10^9 \text{ s}^{-1}$) determined from the slower decay of absorbance at 1030 nm (Fig. 5c). The faster decay of SPA⁺ than the decay of C₆₀⁻ indicates that electron transfer from TPMA to SPA⁺ occurred to produce the CS state (SPA/TPMA⁺/C₆₀⁻), which decayed with the rate constant of $5.7 \times 10^9 \text{ s}^{-1}$ and the CS lifetime of 180 ps. Electron transfer from TPMA to SPA⁺ is indeed energetically feasible, because the one-electron oxidation potential of TPMA (1.20 V vs. SCE) is lower than that of SPA (1.40 V vs. SCE) as shown by their cyclic voltammograms (Fig. S5 in ESI†).

Similarly a transient absorption spectrum of the CS state of SPA/TPMA/C₇₀ was observed by femtosecond laser flash photolysis measurements (Fig. S6 in ESI†). The rate constant of photoinduced electron transfer from ¹SPA* to C₇₀ was determined from the fast decay of absorbance at 600 nm due to ¹SPA* to be $2.6 \times 10^{11} \text{ s}^{-1}$. The CS lifetime of SPA/TPMA⁺/C₇₀⁻ was also determined from the slower decay of absorbance at 1030 nm due to C₇₀⁻ to be $4.4 \times 10^9 \text{ s}^{-1}$, which corresponds to the lifetime of 230

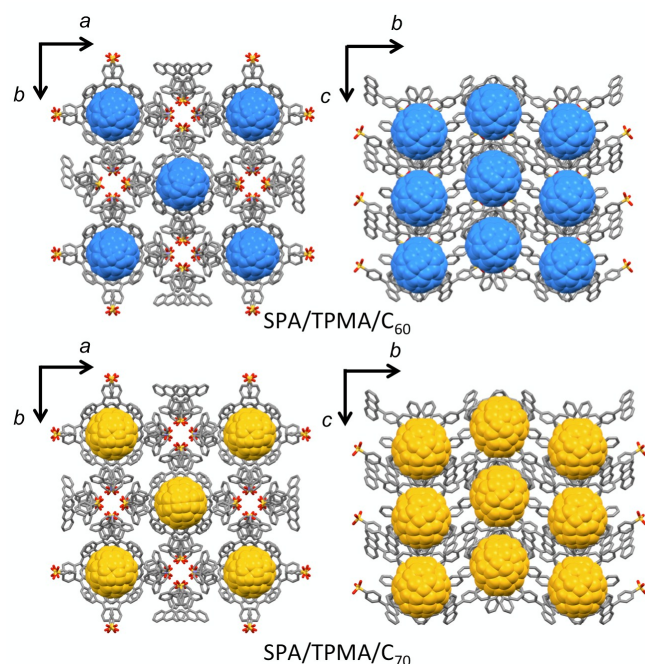


Fig. 2 X-ray crystal structures of SPA/TPMA/C₆₀ (upper panels) and SPA/TPMA/C₇₀ (lower panels).

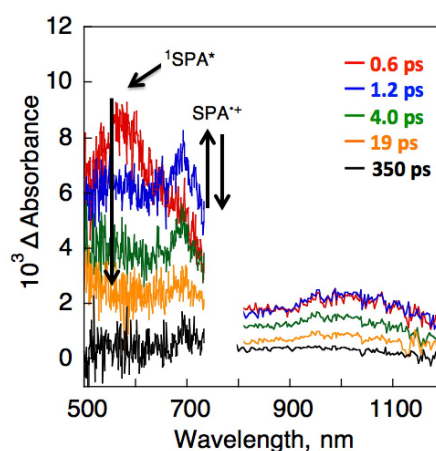


Fig. 4 Transient absorption spectra of SPA/TPMA/C₆₀ dispersed in KBr pellet recorded at 0.6, 1.2, 4.0, 19 and 350 ps after femtosecond laser excitation at 393 nm.

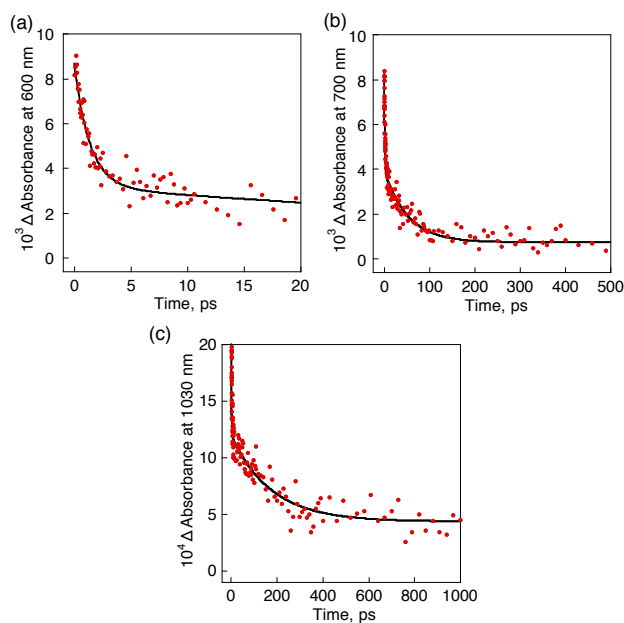


Fig. 5 Decay time profiles of absorption at (a) 600 nm, (b) 700 nm and (c) 1030 nm of SPA/TPMA/C₆₀ in KBr pellet.

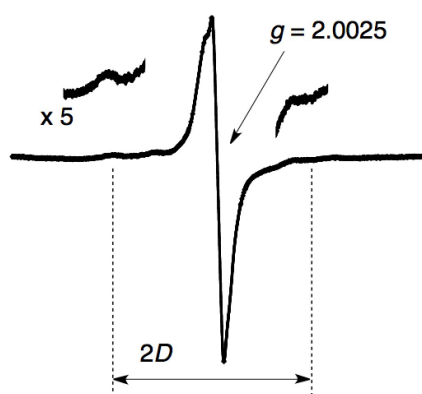


Fig. 6 ESR spectrum observed upon photoirradiation ($\lambda > 340$ nm) of crystals of SPA/TPMA/C₆₀ at 77 K.

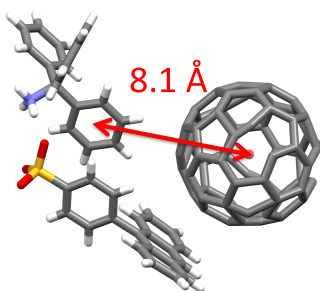


Fig. 7 The centre-to-centre distance between TPMA and C₆₀ in the SPA/TPMA/C₆₀ crystal.

ps.

Upon photoirradiation ($\lambda > 340$ nm) of single crystals of SPA/TPMA/C₆₀ in an ESR cavity at 77 K, we could observe a signal at $g = 2.0025$ as shown in Fig. 6. This signal can be assigned to the superposition of TPMA^{•+} and C₆₀^{•-}. In addition, we could observe a signal due to a triplet CS state, for which the zero-field

splitting (D) value was determined to be 49 G. On the basis of this value, the distance between TPMA^{•+} and C₆₀^{•-} is estimated to be 8.3 Å,²⁴ which is in good agreement with that found in the crystal structure (8.1 Å in Fig. 7).

In conclusion, porous organic salt (POS) crystals composed of 9-(4-sulfophenyl)anthracene (SPA) and triphenylmethylamine (TPMA) were successfully impregnated with fullerenes (C₆₀ and C₇₀) to reveal the X-ray crystal structures. Photoexcitation of POSs impregnated fullerenes resulted in efficient electron transfer from ¹SPA* to fullerenes, followed by hole transfer from SPA^{•+} to TPMA to produce the final CS states (SPA/TPMA^{•+}/C₆₀^{•-} and SPA/TPMA^{•+}/C₇₀^{•-}), which decayed with lifetimes of 180 and 230 ps, respectively. This work has demonstrated the excellent ability of POSs impregnated with fullerenes for efficient photoinduced electron transfer. The tunability and crystalline structures of POSs impregnated with various electron acceptors provide a promising platform to develop artificial photosynthetic systems.

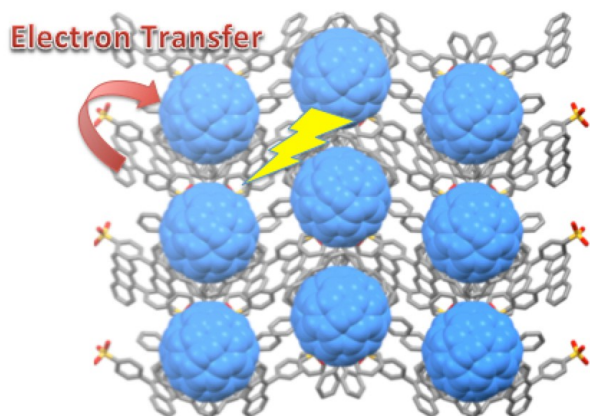
This work was supported by Grants-in-Aid (Nos. 16K13964, 26620154 and 26288037 to K.O.) from the Ministry of Education, Culture, Sports, Science and Technology (MEXT); ALCA and SENTAN project to S.F. from JST, Japan.

Notes and references

- (a) T. Zhang and W. Lin, *Chem. Soc. Rev.*, 2014, **43**, 5982; (b) M. C. So, G. P. Wiederrecht, J. E. Mondloch, J. T. Hupp and O. K. Farha, *Chem. Commun.*, 2015, **51**, 3501; (c) S. Wang and X. Wang, *Small*, 2015, **11**, 3097.
- K. Leong, M. E. Foster, B. M. Wong, E. D. Spoeck, D. Van Gough, J. C. Deaton and M. D. Allendorf, *J. Mater. Chem. A*, 2014, **2**, 3389.
- S. Pullen, H. Fei, A. Orthaber, S. M. Cohen and S. Ott, *J. Am. Chem. Soc.*, 2013, **135**, 16997.
- (a) C. A. Kent, D. Liu, T. J. Meyer and W. Lin, *J. Am. Chem. Soc.*, 2012, **134**, 3991; (b) J.-L. Wang, C. Wang and W. Lin, *ACS Catal.*, 2012, **2**, 2630.
- (a) W. A. Maza and A. J. Morris, *J. Phys. Chem. C*, 2014, **118**, 8803; (b) R. W. Larsen and L. Wojtas, *J. Mater. Chem. A*, 2013, **1**, 14133.
- K. G. M. Laurier, E. Fron, P. Atienzar, K. Kennes, H. Garcia, M. Van der Auweraer, D. E. De Vos, J. Hofkens and M. M. J. Roeflaers, *Phys. Chem. Chem. Phys.*, 2014, **16**, 5044.
- B. Ferrer, M. Alvaro, H. G. Baldovi, H. Reinsch and N. Stock, *ChemPhysChem*, 2014, **15**, 924.
- Y. Zeng, Z. Fu, H. Chen, C. Liu, S. Liao and J. Dai, *Chem. Commun.*, 2012, **48**, 8114.
- L. Han, L. Qin, L.-P. Xu and W.-N. Zhao, *Inorg. Chem.*, 2013, **52**, 1667.
- M. Alvaro, E. Carbonell, B. Ferrer, F. X. Llabrés i Xamena and H. Garcia, *Chem.–Eur. J.*, 2007, **13**, 5106.
- H. Nobukuni, F. Tani, Y. Shimazaki, Y. Naruta, K. Ohkubo, T. Nakanishi, T. Kojima, S. Fukuzumi and S. Seki, *J. Phys. Chem. C*, 2009, **113**, 19694.
- A. I. Cooper, *Angew. Chem., Int. Ed.*, 2012, **51**, 7892.
- (a) P. Li, Y. He, J. Guang, L. Weng, J. C.-G. Zhao, S. Xiang and B. Chen, *J. Am. Chem. Soc.*, 2014, **136**, 547; (b) Y. He, S. Xiang and B. Chen, *J. Am. Chem. Soc.*, 2011, **133**, 14570.
- (a) I. Oueslati, J. A. Paixão, V. H. Rodrigues, K. Suwinska, B. Lesniewska, A. Shkurenko, M. E. S. Eusébio, J. Vicens, T. M. R. Maria and A. L. Ramalho, *Cryst. Growth Des.*, 2013, **13**, 4512; (b) Y.-N. Li, L.-H. Huo, Z.-P. Deng, X. Zou, Z.-B. Zhu, H. Zhao and S. Gao, *Cryst. Growth Des.*, 2014, **14**, 2381.
- (a) A. Comotti, S. Bracco, A. Yamamoto, M. Beretta, T. Hirukawa, N. Tohnai, M. Miyata and P. Sozzani, *J. Am. Chem. Soc.*, 2014, **136**, 618; (b) M. Sugino, K. Hatanaka, Y. Araki, I. Hisaki, M. Miyata and N. Tohnai, *Chem.–Eur. J.*, 2014, **20**, 3069; (c) M. Sugino, K. Hatanaka, T. Miyano, I. Hisaki, M. Miyata, A. Sakon, H. Uekusa and N. Tohnai, *Tetrahedron Lett.*, 2014, **55**, 732.

- 16 (a) Y. Mizobe, M. Miyata, I. Hisaki, Y. Hasegawa and N. Tohnai, *Org. Lett.*, 2006, **8**, 4295; (b) T. Hinoue, M. Miyata, I. Hisaki and N. Tohnai, *Angew. Chem., Int. Ed.*, 2012, **51**, 155.
- 17 (a) M. Sugino, Y. Araki, K. Hatanaka, I. Hisaki, M. Miyata and N. Tohnai, *Cryst. Growth Des.*, 2013, **13**, 4986; (b) A. Yamamoto, T. Hasegawa, T. Hamada, T. Hirukawa, I. Hisaki, M. Miyata and N. Tohnai, *Chem.–Eur. J.*, 2013, **19**, 3006.
- 18 (a) S. Fukuzumi, K. Ohkubo, H. Imahori and D. M. Guldi, *Chem.–Eur. J.*, 2003, **9**, 1585; (b) S. Fukuzumi, T. Suenobu, M. Patz, T. Hirasaka, S. Itoh, M. Fujitsuka and O. Ito, *J. Am. Chem. Soc.*, 1998, **120**, 8060; (c) Y. Kawashima, K. Ohkubo and S. Fukuzumi, *J. Phys. Chem. A*, 2013, **117**, 6737.
- 19 (a) A. Etienne and C. Degent, *FR. Patent* 1085860, Feb 08, 1955; (b) D. P. Getman, G. A. Decrescenzo, J. N. Freskos, M. L. Vazquez, J. A. Sikorski, B. Devadas, S. R. Nagarajan, D. L. Brown and J. J. McDonald, *U.S. Patent* 6388132 Oct 24, 2000.
- 20 (a) N. Tohnai, Y. Mizobe, M. Doi, S. Sukata, T. Hinoue, T. Yuge, I. Hisaki, Y. Matsukawa and M. Miyata, *Angew. Chem., Int. Ed.*, 2007, **46**, 2220; (b) M. Miyata, N. Tohnai and I. Hisaki, *Acc. Chem. Res.*, 2007, **40**, 694.
- 21 (a) A. Yamamoto, S. Uehara, T. Hamada, M. Miyata, I. Hisaki and N. Tohnai, *Cryst. Growth Des.*, 2012, **12**, 4600; (b) A. Yamamoto, T. Hamada, I. Hisaki, M. Miyata and N. Tohnai, *Angew. Chem., Int. Ed.*, 2013, **52**, 1709; (c) A. Yamamoto, T. Hirukawa, I. Hisaki, M. Miyata and N. Tohnai, *Tetrahedron Lett.*, 2013, **54**, 1268.
- 22 UV-vis and fluorescence spectra of SPA/TPMA in PhCN are shown in Fig. S4 in ESI.
- 23 S. Fukuzumi, I. Nakanishi and K. Tanaka, *J. Phys. Chem. A*, 1999, **103**, 11212.
- 24 The distance (r , Å) between the two radical centres was estimated by the following equation: $r = [(2.78 \times 10^4)/D]^{1/3}$.

TOC Graphic



Porous organic salt (POS) crystals composed of 9-(4-sulfophenyl)anthracene and triphenylmethylamine were impregnated with fullerenes (C_{60} and C_{70}), resulting in fluorescence quenching by photoinduced electron transfer.